

PCCP

Accepted Manuscript



This is an *Accepted Manuscript*, which has been through the Royal Society of Chemistry peer review process and has been accepted for publication.

Accepted Manuscripts are published online shortly after acceptance, before technical editing, formatting and proof reading. Using this free service, authors can make their results available to the community, in citable form, before we publish the edited article. We will replace this *Accepted Manuscript* with the edited and formatted *Advance Article* as soon as it is available.

You can find more information about *Accepted Manuscripts* in the [Information for Authors](#).

Please note that technical editing may introduce minor changes to the text and/or graphics, which may alter content. The journal's standard [Terms & Conditions](#) and the [Ethical guidelines](#) still apply. In no event shall the Royal Society of Chemistry be held responsible for any errors or omissions in this *Accepted Manuscript* or any consequences arising from the use of any information it contains.

Multiscale Modeling of Trihexyltetradecylphosphonium Chloride Ionic Liquid

Yong-Lei Wang^{a,b*}, Sten Sarman^c, Bin Li^d, Aatto Laaksonen^{c†}

^a*System and Component Design, Department of Machine Design,
KTH Royal Institute of Technology, SE-100 44 Stockholm, Sweden*

^b*Applied Physical Chemistry, Department of Chemistry,
KTH Royal Institute of Technology, SE-100 44 Stockholm, Sweden*

^c*Department of Materials and Environmental Chemistry,
Arrhenius Laboratory, Stockholm University, SE-106 91 Stockholm, Sweden*

^d*Theoretical Chemistry, Chemical Center, Lund University,
P.O. Box 124, SE-221 00 Lund, Sweden*

(Dated: July 24, 2015)

A multiscale modeling protocol was sketched for the trihexyltetradecylphosphonium chloride ($[P_{6,6,6,14}]Cl$) ionic liquid (IL). The optimized molecular geometry of an isolated $[P_{6,6,6,14}]$ cation and a tightly bound $[P_{6,6,6,14}]Cl$ ion pair structure were obtained from quantum chemistry *ab initio* calculations. A cost-effective united-atom model was proposed for the $[P_{6,6,6,14}]$ cation based on the corresponding atomistic model. Atomistic and coarse-grained molecular dynamics simulations were performed over a wide temperature range to validate the proposed united-atom $[P_{6,6,6,14}]$ model against available experimental data. Through a systemic analysis of volumetric quantities, microscopic structures, and transport properties of the bulk $[P_{6,6,6,14}]Cl$ IL under varied thermodynamic conditions, it was identified that the proposed united-atom $[P_{6,6,6,14}]$ cationic model could essentially capture the local intermolecular structures and the nonlocal experimental thermodynamics, including liquid density, volume expansivity and isothermal compressibility, and transport properties, such as zero-shear viscosity, of the bulk $[P_{6,6,6,14}]Cl$ IL within a wide temperature range.

* E-mail: wangyoni@gmail.com

† E-mail: aatto.laaksonen@mmk.su.se

I. INTRODUCTION

The tetraalkylphosphonium-based ionic liquids (ILs), many of which are composed of volume-occupying alkyl chains, present additional and practical advantages compared with nitrogen-based ILs in large-scale industrial operations due to their remarkable physicochemical properties [1–7]. They are nonflammable, polarity controllable, thermally and electrochemically stable, and have excellent ability to dissolve a large variety of polar and apolar compounds [1, 2, 8, 9]. Moreover, some of them are environmentally benign and commercially available in large quantities, such as tetraalkylphosphonium chloride [10–15], tetraalkylphosphonium chelated orthoborate [16, 17], and tetraalkylphosphonium bis(trifluoromethylsulfonyl)amide [18, 19] ILs, *et al.* [20–22]. These aforementioned desirable and tailorable properties have resulted in their extensive investigations as support media and separating agents in many promising applications in diverse academic and industrial communities, including material synthesis and biocatalysis [1, 4, 23, 24], microfluidics and nanotribology [6, 17, 25], biomass processing [5, 26, 27], liquid phase extraction and gas phase separation (as solvents and membrane transport media) [24, 28–31], as well as in electrochemical devices [32, 33]. Therefore, the number of fundamental studies and industrial applications of tetraalkylphosphonium-based ILs is growing rapidly in recent years [1, 2, 4, 6, 8, 20, 34].

Concerning the current research status of ILs, there is a tremendous amount of combinations of tetraalkylphosphonium cations and different anions with great versatility to tailor their physicochemical properties to meet particular requirements [1, 2, 4, 6, 8, 20, 34]. From an experimental point of view, the traditional trial-and-error way to find appropriate ILs and optimize their functional performance leads to a huge cost on material synthesis and experimental characterizations, and hence it is definitely not feasible to perform experimental tests for all possible ILs one by one. Therefore, it is necessary to establish an economical pre-screening procedure concerning the essential relationship between microscopic structures and macroscopic properties of model IL systems.

Computer simulations, in close interplay with experiments, are well positioned to provide a fundamental understanding of complicated phenomena on molecular level, which is especially useful for ILs because of their tremendous diversity [35–43]. Various simulation methods are available at different length and time scales depending on the specific targets

1 requested from studied IL systems. First-principles quantum mechanics (QM) calculations
2 can provide accurate microstructural information without any experimental support [35, 44–
3 50]. However, due to their computationally demanding nature, these methods are usually
4 adopted to derive effective interactions of ion pairs [35, 46, 50, 51], and to determine delicate
5 interactions with solute molecules in small systems and short time scales [44, 52–54].

6 Molecular simulations on atomistic level are widely used in predicting thermodynamic,
7 structural, and dynamic properties of various IL systems. The quality of atomistic simulation
8 predictions mainly depends on the reliability of the adopted force fields, which refer to the
9 inter- and intramolecular potential parameters used to mimic interactions between atoms in
10 model systems. During the past decades, several atomistic force fields have been developed
11 covering a broad set of phosphonium-based ionic groups by extending and refining available
12 force field parameters [37, 55–57]. These force fields, to some extent, can qualitatively predict
13 physicochemical and structural properties of model ILs compared with experimental data.
14 In our previous work, a high-quality atomistic force field was developed for ILs consisting
15 of the tetraalkylphosphonium cations and the chelated orthoborate anions [57], and vali-
16 dated against available experimental measurements [17]. Furthermore, this proposed force
17 field was extended to study the binary trihexyltetradecylphosphonium bis(oxalato)borate
18 ($[P_{6,6,6,14}][BOB]$) IL/water mixtures with varied water mole fractions [58]. It is particularly
19 observed that the striking thermodynamic quantities and the particular transport proper-
20 ties of studied IL/water mixtures are well connected to the microscopic liquid structural
21 organization and the local ionic environment of the $[P_{6,6,6,14}][BOB]$ IL/water mixtures. The
22 structural and dynamical heterogeneities of the $[P_{6,6,6,14}][BOB]$ IL/water mixtures are ratio-
23 nalized by competition between the favorable interactions between central polar segments in
24 ionic species, and the persistent hydrophobic interactions between alkyl chains in $[P_{6,6,6,14}]$
25 cations.

26 Although much valuable information has been predicted for tetraalkylphosphonium-based
27 ILs through atomistic simulations using accurately developed force field parameters, the cor-
28 rect description of both thermodynamic quantities and transport properties of model ILs
29 comparable with macroscopic experimental measurements is still a challenging task. One
30 critical problem in computational studies is that the bulky and asymmetric tetraalkylphos-
31 phonium cations generally consisting of a large number of atoms, and the strong correlations
32 between ionic groups due to long-range electrostatic interactions, lead to their viscous behav-

ior and thus molecular simulations at large length and long time scales are needed to obtain reliable results. From a computational point of view, good quality coarse-grained models open a possibility to perform extensive simulations with a modest computational cost. In addition to the benefit of computational efficiency, it is also expected that coarse-grained models can reveal essential structural properties of ILs at mesoscopic level by integrating over less important degrees of freedom at atomic scale [39–41, 43, 59, 60].

The united-atom (UA) model is traditionally one of the most popular coarse-graining schemes used to model IL systems [61–64], as well as hydrocarbon systems in general [65, 66]. A cost-effective UA model is usually achieved by lumping several closely bonded atoms into a single interaction site, and the corresponding interaction potentials between UA sites are achieved through empirical parametrization procedures [61–64, 67–69]. Currently, several coarse-graining approaches are available to determine effective interaction potentials between UA sites from atomistic simulation results [39, 59, 61, 63, 65, 68, 70, 71]. Multiscale modeling methodology based on successive coarse-graining schemes is an efficient approach to cover calculations and simulations ranging from nanoscale to mesoscopic level. In the present work, a multiscale modeling protocol unifying QM *ab initio* calculations, atomistic and coarse-grained simulations is sketched for the trihexyltetradecylphosphonium chloride ($[P_{6,6,6,14}]Cl$) IL. The effective interaction potentials derived from QM *ab initio* calculations are fed into atomistic level and then to mesoscale in a self-consistent computational scheme. After the parametrization procedure, both atomistic and coarse-grained simulations are carried out to validate the proposed hierarchical ionic models against available experimental results.

II. MULTISCALE MODELING PROTOCOL

A. Quantum chemistry calculations

The optimized molecular geometry of an isolated $[P_{6,6,6,14}]$ cation and a tightly bound $[P_{6,6,6,14}]Cl$ ion pair structure are obtained from QM *ab initio* calculations using the Gaussian 09 package [72] at B3LYP/6-311++G(d) level without any geometrical constraints. The optimized molecular geometry of the $[P_{6,6,6,14}]$ cation, either in an isolated state or in an ion pair complex, is characterized by a tetrahedral conformation. This particular tetrahedral orientation of four alkyl chains facilitates the approaching of anionic groups to the central

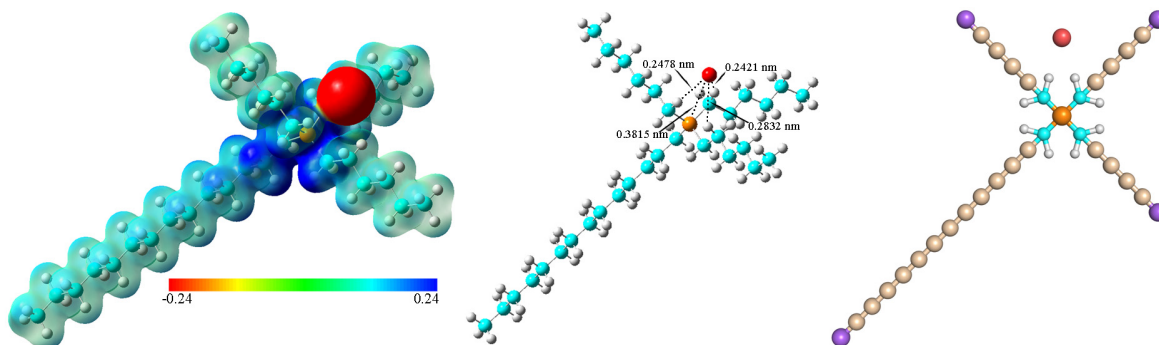


FIG. 1: Left panel: Molecular electrostatic potential surfaces of a tightly bound $[P_{6,6,6,14}]Cl$ ion pair generated from QM *ab initio* calculations. The colored scale bar ranging from -0.24 to 0.24 gives a clear charge distribution in the $[P_{6,6,6,14}]Cl$ ion pair complex. Middle panel: The atomistic $[P_{6,6,6,14}]$ cationic and Cl anionic models with close contacts between the P and HP atoms in the $[P_{6,6,6,14}]$ cation and the Cl anion derived from QM *ab initio* calculations. Right panel: The proposed UA $[P_{6,6,6,14}]$ cationic model and the Cl anion.

1 positive phosphorus (P) atom in the $[P_{6,6,6,14}]$ cation [9, 19, 35, 57, 58]. As the Cl anion
 2 approaches the $[P_{6,6,6,14}]$ cation, it interacts with the hydrogen atoms (marked as HP atoms)
 3 in four methylene CH_2 groups directly connected to the central P atom, resulting in a
 4 cradle-like ionic structure with the Cl anion sitting in the region formed by three alkyl
 5 chains in the $[P_{6,6,6,14}]$ cation, as clearly shown in the left and middle panels of Fig. 1. The
 6 optimized tightly bound $[P_{6,6,6,14}]Cl$ ion pair structure is characterized by strong electrostatic
 7 interactions between the Cl anion and the central P atom, and moderate hydrogen bonded
 8 interactions between the Cl anion and the HP atoms in the $[P_{6,6,6,14}]$ cation, respectively.

9 B. Atomistic ionic models

10 The atomistic force field for the $[P_{6,6,6,14}]$ cation takes the following functional forms for
 11 total potential energy U:

$$\begin{aligned}
 U_{total} = & \sum_{bonds} K_r(r - r_0)^2 + \sum_{angles} K_\theta(\theta - \theta_0)^2 + \sum_{dihedrals} K_\phi[1 + \cos(n\phi - \gamma)] \\
 & + \sum_{i < j} \left\{ 4\epsilon_{ij} \left[\left(\frac{\sigma_{ij}}{r_{ij}} \right)^{12} - \left(\frac{\sigma_{ij}}{r_{ij}} \right)^6 \right] + \frac{q_i q_j}{4\pi\epsilon_0\epsilon_r r_{ij}} \right\}. \quad (1)
 \end{aligned}$$

12 The first three terms represent covalent interactions, *i.e.*, bonds, angles, and dihedrals, and
 13 the corresponding potential parameters have their usual meaning. The non-covalent in-

1 teractions are described in the last term, including van der Waals (vdW) and Coulombic
2 interactions of atom-centered point charges. The interactions separated by exactly three
3 consecutive covalent bonds (1-4 interactions) are reduced by related scaling factors, which
4 are optimized as 0.50 for vdW interactions and 0.83 for electrostatic interactions, respec-
5 tively [38, 57].

6 A set of force field parameters developed for tetraalkylphosphonium cations in our previ-
7 ous work [57] is directly adopted in the present study without further modification. Electro-
8 static polarization effects are not included in atomistic models in order to maintain compu-
9 tational simplicity and transferability of atomistic ionic models to other ILs containing the
10 same ion but different counterions, although the charge density distributions obtained for
11 isolated ions may not necessarily represent their typical configurations in condensed liquid
12 phase with possible partial cancelation in mutual polarization mechanism. The vdW pa-
13 rameters for the Cl anion obtained by fitting the Tosi-Fumi potential [73] can quantitatively
14 describe the microscopic local ionic structure and the hydrogen bond information between
15 imidazolium-based cations and Cl anions [38, 62], and thus are adopted here. The cross
16 interaction parameters between unlike atom types are obtained from the Lorentz-Berthelot
17 combining rules. The force field parameters used for atomistic ionic models are listed in
18 Supporting Information.

19 C. United-atom cationic model

20 The proposed UA $[P_{6,6,6,14}]$ cationic model is shown in the right panel of Fig. 1. The
21 HP atoms in four methylene CH_2 groups directly connected to the central P atom in the
22 atomistic $[P_{6,6,6,14}]$ cation are very different from hydrogen atoms in other methylene CH_2
23 and terminal methyl CH_3 groups, and incline to form hydrogen bonds with the Cl anion as
24 clearly shown in the middle panel of Fig. 1. Therefore, these four methylene CH_2 groups
25 are retained in the UA $[P_{6,6,6,14}]$ model, while the other methylene CH_2 and terminal methyl
26 CH_3 groups are represented as single interaction sites. The force field parameters for the
27 retained atoms in the UA $[P_{6,6,6,14}]$ model are derived from the corresponding atomistic force
28 field without adjustment, and thus have the same potential functional forms as shown in
29 Eq. 1, while the vdW parameters for the united methylene CH_2 and methyl CH_3 sites are
30 adopted from the transferable potentials for phase equilibria (TraPPE) force field developed

1 by the Siepmann group [65, 66].

2 Usually the center of pseudo-UA group was taken from the corresponding carbon atom,
3 and thus the equilibrium bond lengths and angles in atomistic model can be used. However,
4 the center of mass (COM) of UA group does not essentially locate at the carbon center.
5 For example, the COM of methylene CH_2 and methyl CH_3 deviate approximately 0.011 and
6 0.013 nm, respectively, from the corresponding carbon center (shown in Fig. 9). In the
7 present work, the bond lengths between neighboring UA interaction sites are derived from
8 the COM of methylene CH_2 and methyl CH_3 groups instead of using the corresponding
9 carbon atom positions, which, as addressed in previous works [63, 64, 69], could significant-
10 ly improve the prediction of thermodynamic quantities of model ILs. The bond constants
11 K_r are carefully optimized through the method developed by Klein and co-workers [74] in
12 several test simulations so as to reproduce the mean and variance of bond length probability
13 distribution function estimated from atomistic simulations. The angle and dihedral terms
14 are determined in a similar way. The scaling factors for the 1-4 vdW interactions and the
15 1-4 electrostatic interactions are optimized as 0.25 for the UA $[\text{P}_{6,6,6,14}]$ cationic model. Such
16 a coarse-graining procedure, as shown in following discussion, can generally reproduce vol-
17 umetric quantities, microscopic structures, and transport properties of bulk $[\text{P}_{6,6,6,14}]\text{Cl}$ IL.
18 All the optimized force field parameters for the UA $[\text{P}_{6,6,6,14}]$ cationic model are summarized
19 in Supporting Information.

20 Since the motivation of this work is to propose a transferable, computationally efficient,
21 and nonpolarizable UA model for the $[\text{P}_{6,6,6,14}]$ cation through which both thermodynamic
22 and dynamic properties can be reliably predicted, the reduced ion charges are considered as
23 an effective way to account for the average electrostatic polarization effects in condensed liq-
24 uid state. It was shown in previous works that a scaled charge of 0.8e for the UA imidazolium-
25 based cations coupled with different anions gives much better agreement with experimental
26 data [62, 63]. Therefore in the current work, the partial charges for UA sites are determined
27 by simply summing up the atomic charges of their respective atomic constituents, and then
28 scaling the total ion charge as 0.8e for the UA $[\text{P}_{6,6,6,14}]$ cationic model. Correspondingly,
29 the partial ion charge for the Cl anion is rescaled to -0.8e. Although the reduced ion charge
30 of $\pm 0.8e$ for the UA models is just an empirical correction of the average electrostatic polar-
31 ization effects and does not describe varied polarizabilities of ionic groups in different ILs,
32 it gives good performance for the studied $[\text{P}_{6,6,6,14}]\text{Cl}$ IL as verified in following discussion.

D. Simulation methodology

Computer simulations of bulk $[P_{6,6,6,14}]Cl$ IL were performed using the GROMACS 4.6 simulation package [75] with rectangular periodical boundary conditions. The equations of motion were integrated using the classical velocity Verlet leap-frog algorithm with time steps of 1 fs and 2 fs for atomistic and coarse-grained simulations, respectively. The cutoff distance of the vdW interactions and the real-space electrostatic interactions was set to 1.6 nm. The Particle-Mesh Ewald algorithm was employed to handle long-range electrostatic interactions in the reciprocal space with a FFT grid spacing of 0.12 nm and an accuracy of 10^{-5} , respectively. All simulation systems were first annealed gradually from 600 K down to target temperatures (273, 293, 313, 333, 353, 373, and 393 K) within 4 ns maintained using a Nosé-Hoover thermostat coupled with an anisotropic Parrinello-Rahman barostat under 1 atm with time coupling constants of 200 and 500 fs to control temperature and pressure, respectively.

Both atomistic and coarse-grained simulation systems are composed of 128 and 512 $[P_{6,6,6,14}]Cl$ ion pairs, respectively. These simulation systems were equilibrated in isothermal isobaric ensemble for 10 ns and 20 ns, respectively, at varied temperatures to obtain ensemble-averaged volumetric quantities. Subsequently, atomistic and coarse-grained simulations were performed in canonical ensemble for another 40 ns and 80 ns with comparable computational times, respectively, in which simulation trajectories were recorded with an interval of 100 fs for further analysis.

III. RESULTS AND DISCUSSION

A. Volumetric quantities

Experimental liquid densities are the most frequently used sources to validate proposed force field parameters, as liquid density values can be easily obtained from isothermal isobaric simulations. In the present work, the liquid densities of $[P_{6,6,6,14}]Cl$ IL at varied temperatures ranging from 273 to 393 K are calculated based on atomistic and coarse-grained force field parameters, respectively, and the corresponding simulation results are compared with available experimental data [11–14] and shown in Fig. 2.

The predicted liquid densities of bulk $[P_{6,6,6,14}]Cl$ IL, based on either atomistic or UA

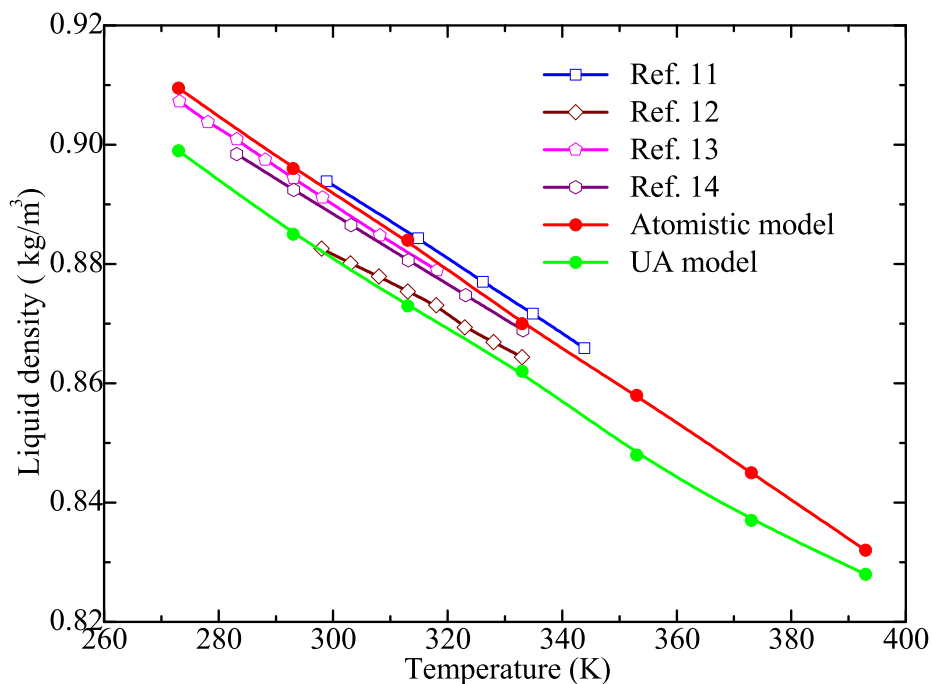


FIG. 2: Liquid densities of bulk $[P_{6,6,6,14}]Cl$ IL calculated from atomistic and UA models as a function of temperature and compared with experimental data [11–14].

1 force field parameters, exhibit linear variations within the investigated temperature range of
 2 273 – 393 K, and are in remarkably good agreement with available experimental results [11–
 3 14]. The largest absolute relative deviation between atomistic simulations and experimental
 4 measurements is approximately 1.5%, and the coarse-grained simulation results deviate less
 5 than 2.5% from experimental data, respectively. This is reasonable since the equilibrium
 6 bond lengths and angle distributions in the UA $[P_{6,6,6,14}]$ cationic model are accurately
 7 obtained from the COM of the corresponding methylene CH_2 and methyl CH_3 groups in the
 8 atomistic $[P_{6,6,6,14}]$ model. Such a coarse-graining procedure, as shown in previous works [63,
 9 64, 69], can generally reproduce good liquid density predictions of the corresponding model
 10 IL systems.

11 The volume expansivity, defined as $\alpha_P = \frac{1}{V}(\frac{\partial V}{\partial T})_P$, quantifies the dependence of a fluid
 12 volumetric change on temperature. In the present work, the volume expansivity values of
 13 bulk $[P_{6,6,6,14}]Cl$ IL at atmospheric pressure are calculated from atomistic and coarse-grained
 14 simulations, and thereafter compared with experimental measurements deduced from pre-
 15 vious studies [12, 13, 15] and shown in Fig. 3. Apparently, the isobaric volume expansion
 16 coefficients of bulk $[P_{6,6,6,14}]Cl$ IL calculated from atomistic models are in agreement with

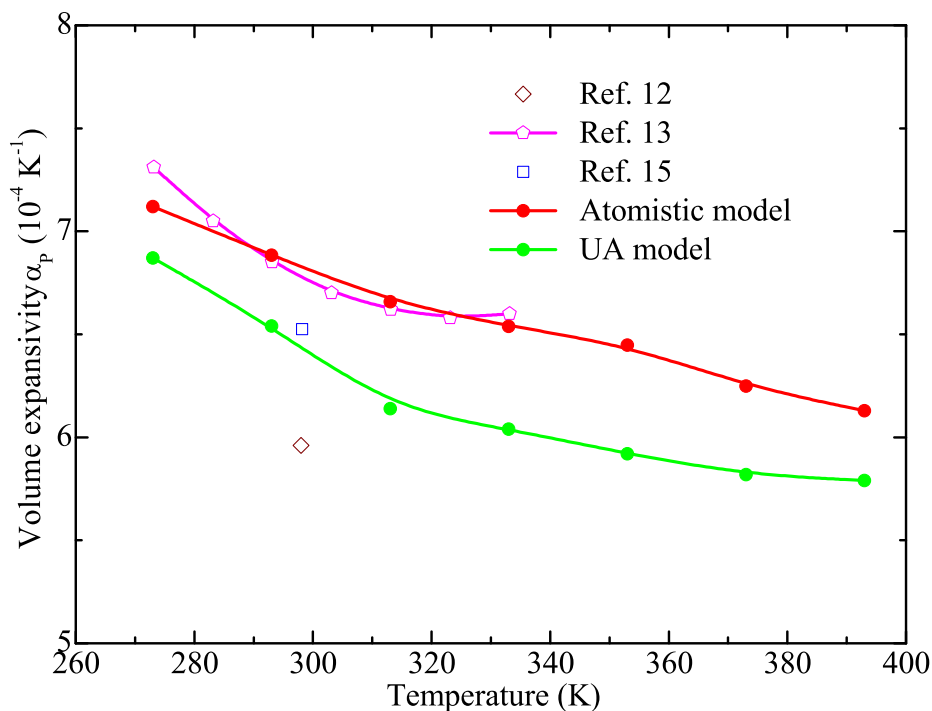


FIG. 3: Isobaric volume expansion coefficients α_P of bulk $[P_{6,6,6,14}]Cl$ IL calculated from atomistic and UA models as a function of temperature and compared with experimental data [12, 13, 15].

1 available experimental results within the investigated temperature range of 273 – 393 K.
 2 However, some non-negligible discrepancies are observed for α_P values calculated from UA
 3 models compared with atomistic simulation results and experimental data. Concerning the
 4 lack of some intramolecular degrees of freedom in the proposed UA $[P_{6,6,6,14}]$ cationic model,
 5 it is reasonable to point out that the isobaric volume expansion coefficients estimated from
 6 coarse-grained simulations are generally acceptable as these α_P data still lie within typical
 7 experimental range for bulk $[P_{6,6,6,14}]Cl$ IL.

8 Fig. 4 presents the calculated isothermal compressibility data, described as $\kappa_T =$
 9 $-\frac{1}{V}(\frac{\partial V}{\partial P})_T$, of bulk $[P_{6,6,6,14}]Cl$ IL estimated from current atomistic and coarse-grained simu-
 10 lations, as well as experimental results derived from previous works [10, 13, 14]. The isother-
 11 mal compressibility results estimated from atomistic simulations are consistently lower than
 12 experimental values by 12% – 21%, while the ones predicted from coarse-grained simulations
 13 are uniformly larger than those obtained from experimental measurements by 51% – 59%,
 14 respectively. This level of discrepancy is qualitatively reasonable, especially considering
 15 some non-negligible impurities in experimentally studied $[P_{6,6,6,14}]Cl$ IL samples [10, 13, 14],

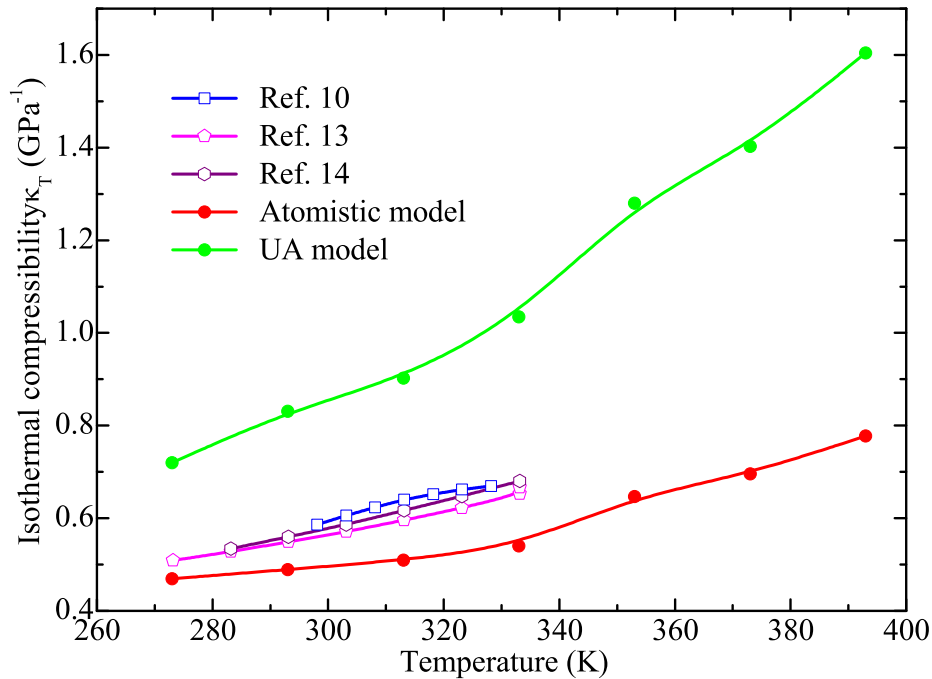


FIG. 4: Isothermal compressibility coefficients κ_T of bulk $[P_{6,6,6,14}]Cl$ IL calculated from atomistic and UA models as a function of temperature and compared with experimental data [10, 13, 14].

1 and computationally difficulties in calculating pressures from atomistic and coarse-grained
 2 simulations. In addition, the reduction of some intramolecular degrees of freedom in the
 3 proposed UA $[P_{6,6,6,14}]$ cationic model contributes to the larger isothermal compressibility
 4 coefficients as compared to the experimental data and the atomistic simulation results.

5

B. Microscopic structures

6 The site-site radial distribution function (RDF) quantifies spatial correlations between
 7 specific atoms and other similar or dissimilar atoms in their surrounding environment [37, 57,
 8 62], which is useful for the concretization of local microscopic ionic structure between ionic
 9 species. In the present work, the RDFs calculated from UA models are compared with those
 10 deduced from the corresponding atomistic models to assess the accuracy of the proposed
 11 UA models in predicting local ionic structure of bulk $[P_{6,6,6,14}]Cl$ IL. The central P atoms,
 12 both in the atomistic and in the UA $[P_{6,6,6,14}]$ cationic models, are taken as reference sites to
 13 calculate the corresponding site-site RDFs. Typical RDFs for cation-cation, cation-anion,
 14 and anion-anion pairs of $[P_{6,6,6,14}]Cl$ IL based on both atomistic and UA models at 333 K

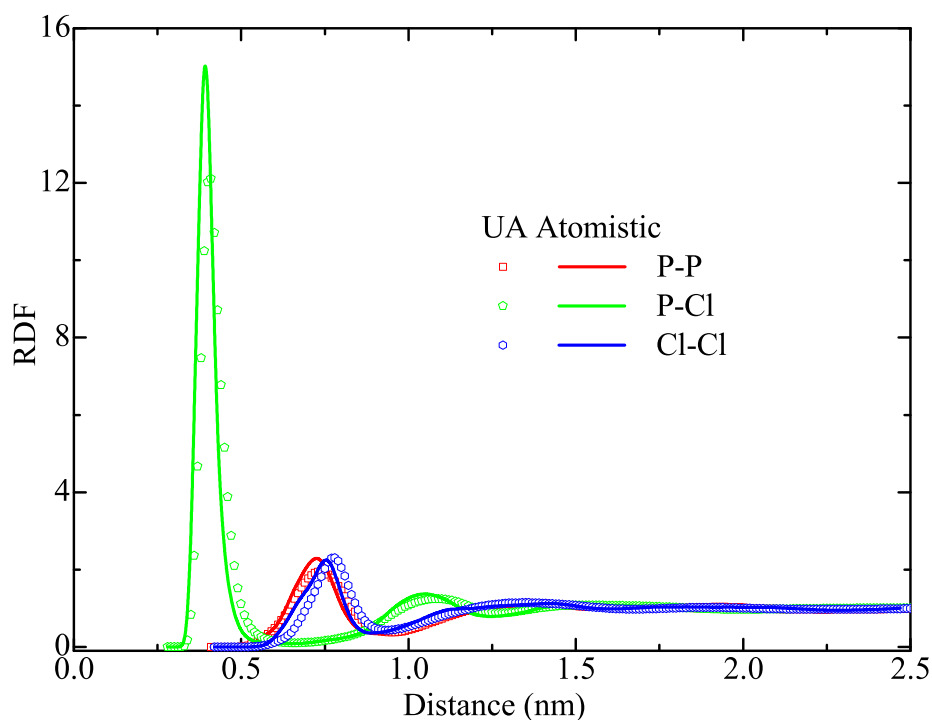


FIG. 5: Typical radial distribution functions of cation-cation, cation-anion, and anion-anion pairs calculated from atomistic and UA $[P_{6,6,6,14}]$ cations and Cl anions at 333 K. The central P atoms, both in the atomistic and in the UA $[P_{6,6,6,14}]$ cationic models, are taken as reference sites to calculate the corresponding RDFs.

1 are presented in Fig. 5.

2 As a rough description of local ionic structure given by site-site RDFs, it is observed that
3 three set of RDFs calculated from UA models agree remarkably well with that exhibited
4 by atomistic representations. The sharp peak registered at approximately 0.40 nm in the
5 P-Cl RDFs indicates a well-organized ionic structure with a distinct first coordination shell
6 of Cl anions around $[P_{6,6,6,14}]$ cations due to strong electrostatic interactions. The marginal
7 difference lies in secondary peaks in three RDFs, in which the ones deduced from UA models
8 are much smoother than those obtained from the corresponding atomistic counterparts. This
9 phenomenon may originate from the simpler molecular shape and the absence of some minor
10 conformational degrees of freedom in the proposed UA $[P_{6,6,6,14}]$ cationic model. It is well-
11 known that some minor structural features in atomistic model are averaged out during the
12 coarse-graining procedure of lumping several closely bonded atoms into a single interaction
13 site, resulting in the corresponding UA model exhibits less steric effects and hence leads to

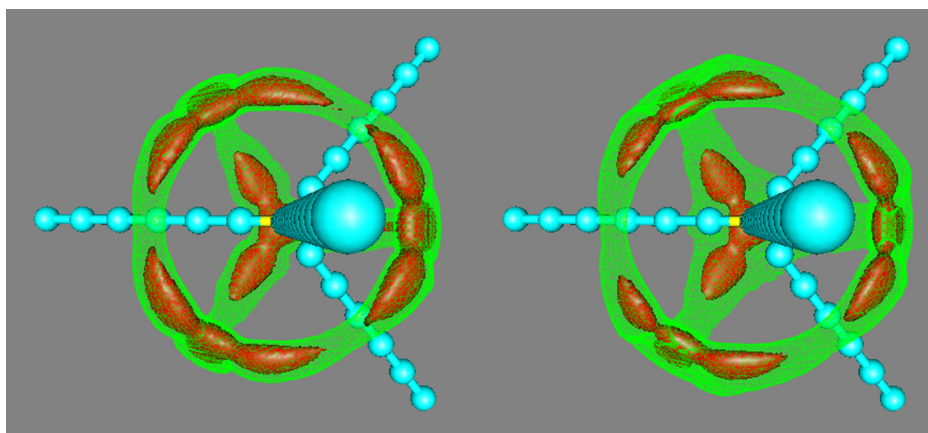


FIG. 6: Three-dimensional probability distributions of Cl anions around atomistic (left panel) and UA (right panel) $[P_{6,6,6,14}]$ cations obtained from current simulations at 333 K. The red solid and green meshed bounded contour surfaces are drawn at 8.0 and 4.0 times of the average density of Cl anions, respectively. The phosphorus and carbon atoms in the $[P_{6,6,6,14}]$ cation are represented by yellow and cyan beads in the skeleton, respectively.

1 less sharpening features in secondary RDF peaks. Such an observation is generally consistent
2 with that reported in the UA models for imidazolium-based cations [61, 62, 69]. Additionally,
3 the calculated cation-cation, cation-anion, and anion-anion pair RDFs from UA models at
4 other temperatures show qualitatively similar features as those obtained from atomistic
5 simulations, and are hence not shown here.

6 In addition to these spherically averaged RDFs, the microscopic liquid structure of bulk
7 $[P_{6,6,6,14}]Cl$ IL can be further illustrated by spatial distribution function (SDF), giving the
8 probability of finding a specific atom around a central molecule in three-dimensional s-
9 pace [37, 38, 57]. In the present work, all SDFs are visualized using the gOpenMol pack-
10 age [76, 77]. Fig. 6 presents typical SDFs of Cl anions around a $[P_{6,6,6,14}]$ cation calculated
11 from atomistic and coarse-grained simulations at 333 K, respectively. As expected, Cl anions
12 coordinate with $[P_{6,6,6,14}]$ cations in a tetrahedral region due to strong electrostatic inter-
13 actions and distinct steric effects of four alkyl substituents in $[P_{6,6,6,14}]$ cations. The four
14 preferred high probability domains contribute to the first solvation shell in the corresponding
15 RDFs shown in Fig. 5. This observation is similar to the spatial distributions of chelated
16 orthoborate anions and water molecules around tetraalkylphosphonium cations reported in
17 our previous works [57, 58].

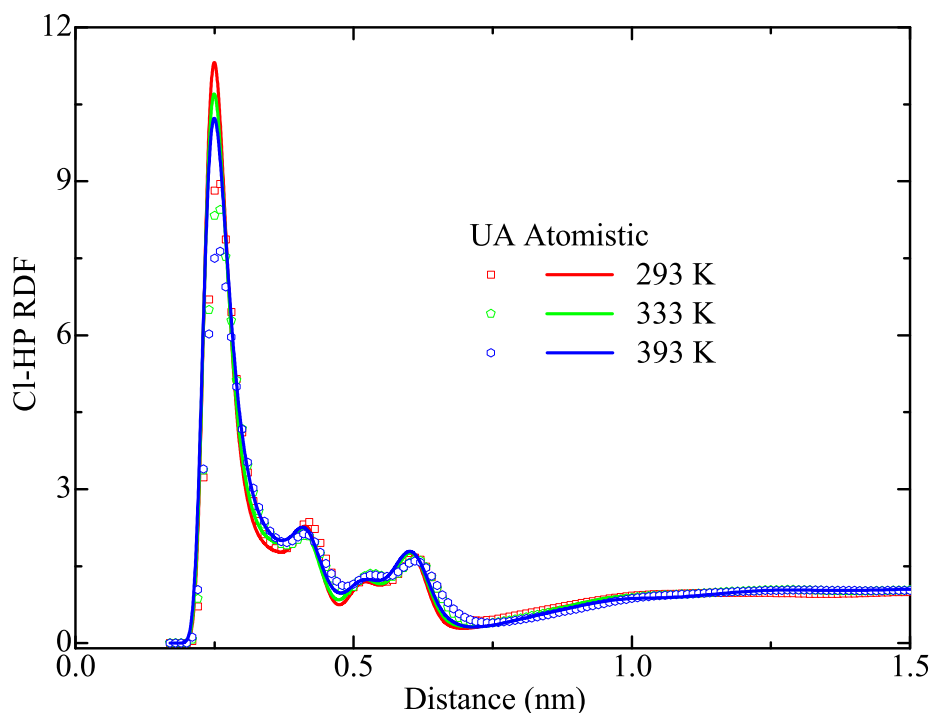


FIG. 7: Typical radial distribution functions between Cl anions and the HP atoms in atomistic and UA $[P_{6,6,6,14}]$ cations at 293, 333, and 393 K, respectively.

1 It was suggested in previous studies that different anionic groups preferentially interact
2 with the HP atoms in $[P_{6,6,6,14}]$ cations due to their expected hydrogen bonded interac-
3 tions [35, 37, 56–58]. Fig. 7 presents the site-site Cl-HP RDFs calculated from atomistic
4 and coarse-grained simulations at 293, 333, and 393 K, respectively. A sharp and intense
5 peak registered at approximately 0.25 nm contributes to the formation of hydrogen bonds
6 between the HP atoms in $[P_{6,6,6,14}]$ cations and the Cl anionic groups, which is consistent
7 with previous experimental NMR spectroscopic studies [78–81] and the electronic structure
8 calculation [9, 35, 78] of the $[P_{6,6,6,14}]$ -based ILs. The three secondary peaks character-
9 ized with less peak intensities are observed at larger distances. The RDF peak positions and
10 plot shapes calculated from UA models coincide very well with those deduced from the
11 corresponding atomistic counterparts, indicating that the local hydrogen bond structure is
12 retained in the cost-effectively refined UA $[P_{6,6,6,14}]$ cationic model.

13 Due to the relative central position of the HP atoms and large volume of the $[P_{6,6,6,14}]$
14 cation, it is difficult to visualize the three-dimensional probability distribution of Cl anions
15 around the HP atoms [57, 58]. Herein, we present a combined distribution function (CDF)

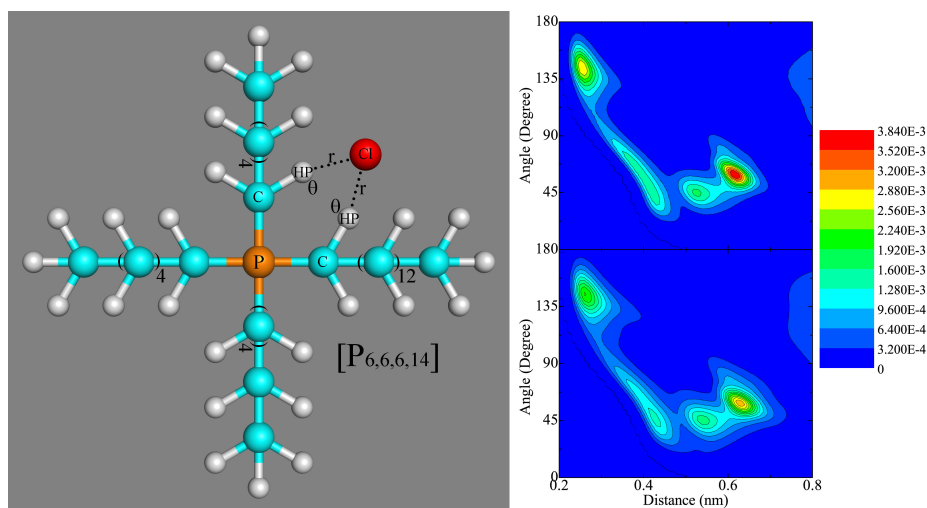


FIG. 8: Left panel: Schematic description of the Cl \cdots HP-C angle θ and the Cl \cdots HP distance r . Right panel: Combined distribution function of the Cl \cdots HP-C angle versus the Cl \cdots HP distance calculated from atomistic (top) and UA (bottom) models at 333 K, respectively.

1 of the Cl \cdots HP-C angle versus the Cl \cdots HP distance in Fig. 8. There are four distinct
 2 coordination regions of Cl anions with the HP atoms in [P_{6,6,6,14}] cations, mirroring the four
 3 particular peaks exhibited in the corresponding Cl-HP RDFs. The first region registered at
 4 $120^\circ < \theta < 165^\circ$ (the Cl \cdots HP-C angle) and $0.23 \text{ nm} < r < 0.30 \text{ nm}$ (the Cl \cdots HP distance)
 5 indicates that Cl anions are strongly hydrogen bonded to the HP atoms, both in atomistic
 6 and in UA [P_{6,6,6,14}] cationic models.

7 Besides the microscopic ionic and hydrogen bond structures, the conformation of alkyl
 8 substituents in the UA [P_{6,6,6,14}] cationic model is investigated by examining the equilib-
 9 rium bond lengths between neighboring UA interaction sites and the equilibrium angles
 10 among three consecutive UA beads. The bond length (CH₂-CH₂ and CH₂-CH₃) and angle
 11 (CH₂-CH₂-CH₂ and CH₂-CH₂-CH₃) probability distributions shown in the left and middle
 12 panels of Fig. 9 indicate that the proposed UA [P_{6,6,6,14}] cationic model can precisely “repro-
 13 duce” the average bond lengths and angles determined from the corresponding atomistic
 14 model. Additionally, the RDFs of terminal carbon atoms of the hexyl and tetradecyl chains
 15 in UA [P_{6,6,6,14}] cationic model are qualitatively consistent with that determined from the
 16 atomistic one. Combining all these RDF, SDF, CDF, and probability distribution analyses,
 17 we can specify that the proposed UA [P_{6,6,6,14}] cationic model can essentially capture the
 18 intrinsic microscopic ionic structure of bulk [P_{6,6,6,14}]Cl IL as accurately as the atomistic

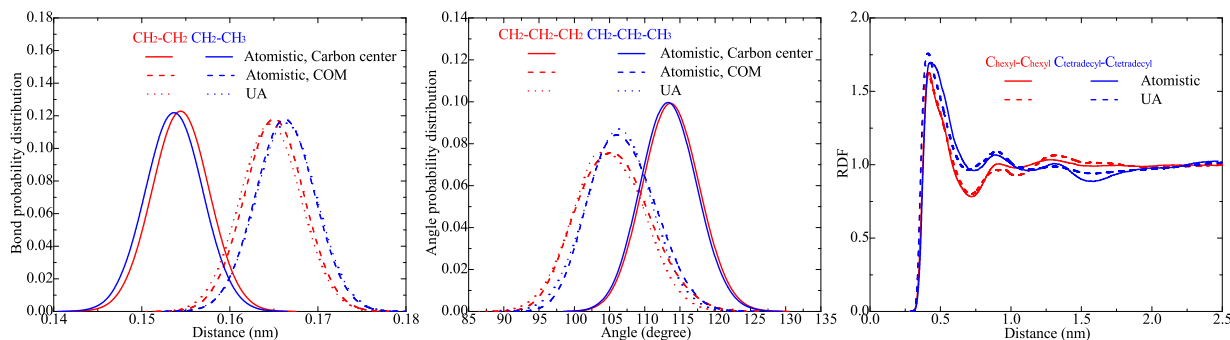


FIG. 9: The bond length (left panel) and angle (middle panel) probability distributions calculated from the proposed UA [P_{6,6,6,14}] cationic model are compared with the ones determined from the atomistic model. Right panel: Radial distribution functions of the terminal carbon atoms in alkyl chains of the proposed UA [P_{6,6,6,14}] cationic model are compared with the ones calculated from the atomistic model.

1 model does.

2 C. Transport properties

3 The self-diffusivity refers to the translational and rotational motion of liquid molecules
 4 initiated by systematic thermal agitation of surrounding molecules under thermodynamic
 5 equilibrium conditions [68, 82]. From a molecular point of view, the self-diffusivity of liquid
 6 molecules gives a detailed microscopic description of single-particle motion. In the present
 7 work, single-particle dynamics of ionic species are characterized by calculating their respec-
 8 tive translational self-diffusion coefficients, which represent the ability of a molecule to move
 9 inside its surrounding environment. The calculation of translational self-diffusion coeffi-
 10 cients of ionic species is relatively straightforward from the recorded simulation trajectories
 11 through the well-known Einstein formula [41, 62, 63, 82]:

$$D = \frac{1}{6} \lim_{t \rightarrow \infty} \frac{d}{dt} \langle |\mathbf{r}_i^c(t) - \mathbf{r}_i^c(0)|^2 \rangle, \quad (2)$$

12 where the quantity $\langle |\mathbf{r}_i^c(t) - \mathbf{r}_i^c(0)|^2 \rangle$ represents an ensemble-averaged mean square displace-
 13 ment, and $\mathbf{r}_i^c(t)$ the COM vector coordinate of the i th ionic group at time t . The diffusion
 14 coefficient is determined by a linear fitting of the slope of an ensemble-averaged mean square
 15 displacement in typical diffusive regime.

TABLE I: Translational diffusion coefficients (in 10^{-12} m²/s) of atomistic and UA [P_{6,6,6,14}] cations and Cl anions calculated from atomistic and coarse-grained simulations at varied temperatures, respectively.

Temperature (K)	Atomistic simulations		Coarse-grained simulations	
	[P _{6,6,6,14}] cations	Cl anions	[P _{6,6,6,14}] cations	Cl anions
273	0.71(0.13)	0.34(0.11)	1.59(0.15)	0.62(0.12)
293	1.51(0.29)	0.79(0.24)	2.09(0.27)	1.08(0.21)
313	2.49(0.35)	1.31(0.32)	3.38(0.41)	1.61(0.32)
333	3.23(0.61)	1.58(0.39)	4.81(0.53)	2.23(0.48)
355	5.14(0.88)	2.12(0.45)	7.87(0.87)	3.88(0.76)
373	9.12(1.11)	4.21(0.61)	12.82(1.12)	8.07(1.12)
393	18.18(1.53)	7.55(0.92)	25.26(1.78)	14.56(1.53)

1 The temperature dependence of translational diffusion coefficients of [P_{6,6,6,14}] cations and
 2 Cl anions obtained from atomistic and coarse-grained simulations are listed in Table I. A
 3 general feature is that the mobility of ionic species increases exponentially as temperature
 4 increases, both for atomistic and UA [P_{6,6,6,14}] cations, and for Cl anions in atomistic and
 5 coarse-grained simulations, respectively. Upon further inspection of these diffusion coeffi-
 6 cient data, it is found that the bulky, asymmetrical and larger [P_{6,6,6,14}] cations diffuse much
 7 faster than the spherical and smaller Cl anions, both in atomistic and in coarse-grained sim-
 8 ulations, respectively. It is noteworthy that similar diffusion features have been reported in
 9 coarse-grained simulations of imidazolium-based ILs compared with the corresponding atom-
 10 istic simulations and with related experimental NMR measurements [38, 40, 41, 62, 63, 83].
 11 These diffusion features in current atomistic and coarse-grained simulations can be attribut-
 12 ed to the strong electrostatic interactions and the specific hydrogen bonded interactions
 13 between [P_{6,6,6,14}] cations and Cl anions, leading to the constrained distribution of Cl anions
 14 in tetrahedral regions formed by four alkyl substituents in [P_{6,6,6,14}] cations, as well as their
 15 slaved diffusion in confined space.

16 Due to the scarcity of diffusion coefficient data of [P_{6,6,6,14}]Cl IL in literature, it is diffi-
 17 cult to make a direct comparison of our simulation results with experimental measurements.
 18 Herein we mainly focus on the comparison of diffusion data calculated from atomistic and

1 coarse-grained simulations under varied thermodynamic conditions. It is shown that the
 2 diffusivities of [P_{6,6,6,14}] cations and Cl anions estimated from coarse-grained simulations
 3 are approximately 1 – 2 folds larger than the corresponding counterparts determined from
 4 atomistic simulations over the entire temperature range studied here. The deviation of
 5 translational diffusion coefficients may be attributed to the simplification of the atomistic
 6 [P_{6,6,6,14}] cation by removing partial degrees of freedom, and thereafter the determined ef-
 7 fective interaction potentials, leading to a softer repulsion between UA interaction sites and
 8 consequently to a faster diffusion [40, 41, 43, 62, 63].

9 Despite the lack of diffusion coefficient data from experiments, the current atomistic and
 10 coarse-grained simulations can provide valuable insights into some other dynamical quanti-
 11 ties, such as the zero-shear viscosity of bulk [P_{6,6,6,14}]Cl IL. Compared with the calculation
 12 of self-diffusivity of liquid molecules, the evaluation of zero-shear viscosity from molecu-
 13 lar simulations is a challenging task since it is a collective property describing a dissipative
 14 transport process in model system [41, 62–64]. The accuracy of evaluating zero-shear viscos-
 15 ity of a model system cannot be statistically improved by averaging over all liquid molecules
 16 within the simulation scheme but increasing simulation time. For IL systems, the long re-
 17 laxation time of ionic species caused by strong long-range electrostatic interactions leads to
 18 the evaluation of zero-shear viscosity even more time consuming. In the present work, the
 19 zero-shear viscosity is evaluated via equilibrium molecular dynamics simulations through
 20 the Green-Kubo formula [41, 62–64, 84]:

$$\eta = \frac{V}{10k_B T} \int_0^\infty \langle \sum_{\alpha\beta} \bar{P}_{\alpha\beta}(t) \bar{P}_{\alpha\beta}(0) \rangle dt, \quad (3)$$

21 where V is the volume of simulation cell, k_B the Boltzmann constant, and T the absolute
 22 temperature, respectively. $\bar{P}_{\alpha\beta}$ is the off-diagonal element of symmetric traceless pressure
 23 tensor $\sigma_{\alpha\beta}$, and is defined as:

$$\bar{P}_{\alpha\beta} = \frac{1}{2}(\sigma_{\alpha\beta} + \sigma_{\beta\alpha}) - \frac{1}{3}\delta_{\alpha\beta}(\sum_{\gamma} \sigma_{\gamma\gamma}), \quad (4)$$

24 in which $\delta_{\alpha\beta}$ is the Kronecker delta function and $\delta = 1$ when $\alpha = \beta$; otherwise, $\delta = 0$.

25 The predicted zero-shear viscosities of bulk [P_{6,6,6,14}]Cl IL from coarse-grained simulations
 26 are present in Fig. 10 along with available experimental data deduced from previous work-
 27 s [11, 15, 85]. It is shown that the zero-shear viscosities of bulk [P_{6,6,6,14}]Cl IL estimated from
 28 coarse-grained simulations agree in general with available experimental results, even little

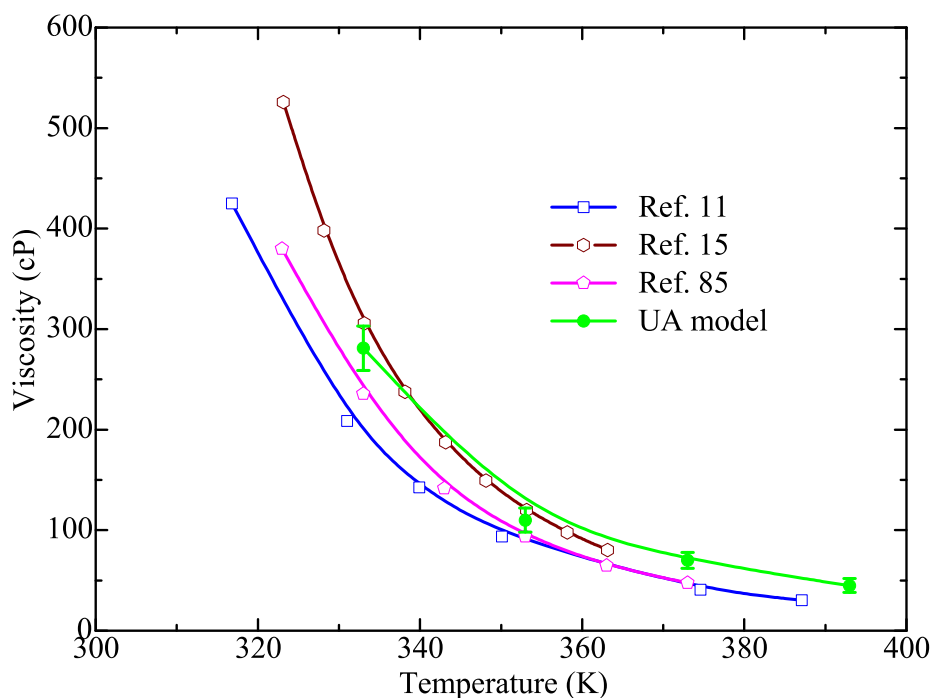


FIG. 10: Temperature dependence of zero-shear viscosities of bulk $[P_{6,6,6,14}]Cl$ IL predicted from current coarse-grained simulations and compared with experimental data [11, 15, 85].

1 overestimation is observed at high temperatures. Such overestimations are also present in
 2 UA models for imidazolium-based cations with varied deviations ranging from 50% to 200%
 3 reported in previous works [62, 63]. However, the prediction of zero-shear viscosities from
 4 atomistic simulations is not converged within a limited simulation time, *e.g.* 40 ns in current
 5 atomistic simulations, because of the overall sluggish dynamics of the neat $[P_{6,6,6,14}]Cl$ IL.

6 Concerning the extensive analyses of volumetric quantities, microscopic structures, and
 7 transport properties of the model $[P_{6,6,6,14}]Cl$ IL against available experimental data, it is
 8 identified that the proposed UA $[P_{6,6,6,14}]$ cationic model can essentially capture general
 9 physicochemical properties of bulk $[P_{6,6,6,14}]Cl$ IL within the investigated temperature range
 10 as accurately as the atomistic $[P_{6,6,6,14}]$ model does. As such, the proposed UA $[P_{6,6,6,14}]$
 11 cationic model can be regarded as a step towards a general coarse-grained force field for
 12 tetraalkylphosphonium cations that will be built in a coherent way in future works.

IV. CONCLUSIONS

In the present work, a complete multiscale modeling protocol was sketched for the $[P_{6,6,6,14}]Cl$ IL, in which the force field parameters derived at high-resolution scale are transferred to low-resolution level in a self-consistent computational scheme using a bottom-up approach bridging different length and time scales. Quantum mechanical *ab initio* calculations were first performed to obtain the optimized molecular geometries of an isolated $[P_{6,6,6,14}]$ cation and a tightly bound $[P_{6,6,6,14}]Cl$ ion pair structure. The effective force field parameters and atomic partial charges for the atomistic $[P_{6,6,6,14}]$ cation were proposed in our previous work. Furthermore, an economical and nonpolarizable UA model was constructed for the $[P_{6,6,6,14}]$ cation. The interaction parameters for UA sites were carefully fine-tuned to qualitatively match atomistic force field parameters. A reduced partial charge of $\pm 0.8e$ was used in UA models as an effective way to account for the average electrostatic polarization effects in condensed liquid state.

Atomistic and coarse-grained molecular dynamics simulations were performed over a wide temperature range of 273 – 393 K to validate the proposed ionic models against available experimental data. The predicted volumetric quantities, including liquid density, volume expansivity and isothermal compressibility, of bulk $[P_{6,6,6,14}]Cl$ IL agree well with available experimental measurements reported in literatures. The combination of RDFs, SDFs, CDFs, and bond length and angle probability distributions reveals that the proposed UA $[P_{6,6,6,14}]$ cationic model can essentially depict the microscopic liquid structure and the local ionic environment of bulk $[P_{6,6,6,14}]Cl$ IL. The calculated zero-shear viscosities of $[P_{6,6,6,14}]Cl$ IL based on UA models from coarse-grained simulations are generally consistent with experimental data with relative small deviations in a reasonable range.

In summary, through a systemic analysis of volumetric quantities, microscopic structures, and transport properties of bulk $[P_{6,6,6,14}]Cl$ IL under varied thermodynamic conditions, it is identified that the proposed UA $[P_{6,6,6,14}]$ cationic model can essentially capture the intrinsic local intermolecular structure predicted by *ab initio* calculations and atomistic simulations, and the nonlocal thermodynamic and transport properties against the corresponding experimental measurements of $[P_{6,6,6,14}]Cl$ IL over a wide temperature range. From a perspective point of view, the multiscale modeling protocol proposed here to construct atomistic and UA models from *ab initio* calculations is useful and can be extended to other classes of

1 ILs. Following the approach presented in the current study, the transferability of force field
2 parameters to other tetraalkylphosphonium cations with varied alkyl chain lengths will be
3 investigated in future works.

4 Acknowledgment

5 We gratefully acknowledge financial support from the Knut and Alice Wallenberg Foun-
6 dation and the Swedish Research Council. All computer simulations were performed using
7 computational resources provided by the Swedish National Infrastructure for Computing
8 (SNIC) at PDC, HPC2N and NSC.

-
- 9 [1] N. V. Plechkova and K. R. Seddon, *Chem. Soc. Rev.* **37**, 123 (2008).
10 [2] K. J. Fraser and D. R. MacFarlane, *Aust. J. Chem.* **62**, 309 (2009).
11 [3] E. W. Castner Jr, C. J. Margulis, M. Maroncelli, and J. F. Wishart, *Annu. Rev. Phys. Chem.*
12 **62**, 85 (2011).
13 [4] J. P. Hallett and T. Welton, *Chem. Rev.* **111**, 3508 (2011).
14 [5] H. Wang, G. Gurau, and R. D. Rogers, *Chem. Soc. Rev.* **41**, 1519 (2012).
15 [6] A. E. Somers, P. C. Howlett, D. R. MacFarlane, and M. Forsyth, *Lubricants* **1**, 3 (2013).
16 [7] S. Zhang, J. Sun, X. Zhang, J. Xin, Q. Miao, and J. Wang, *Chem. Soc. Rev.* **43**, 7838 (2014).
17 [8] R. E. Del Sesto, C. Corley, A. Robertson, and J. S. Wilkes, *J. Organomet. Chem.* **690**, 2536
18 (2005).
19 [9] S. Zahn and A. Stark, *Phys. Chem. Chem. Phys.* **17**, 4034 (2015).
20 [10] J. M. S. S. Esperança, H. J. R. Guedes, M. Blesic, and L. P. N. Rebelo, *J. Chem. Eng. Data*
21 **51**, 237 (2006).
22 [11] J. W. Vaughan, D. Dreisinger, and J. Haggins, *ECS Trans.* **2**, 381 (2006).
23 [12] P. Kilaru, G. A. Baker, and P. Scovazzo, *J. Chem. Eng. Data* **52**, 2306 (2007).
24 [13] F. Goncalves, C. Costa, C. Ferreira, J. Bernardo, I. Johnson, I. Fonseca, and A. Ferreira, *J.*
25 *Chem. Thermodyn.* **43**, 914 (2011).
26 [14] L. I. N. Tomé, R. L. Gardas, P. J. Carvalho, M. J. Pastoriza-Gallego, M. M. Pineiro, and
27 J. A. P. Coutinho, *J. Chem. Eng. Data* **56**, 2205 (2011).

- 1 [15] C. M. Neves, P. J. Carvalho, M. G. Freire, and J. A. Coutinho, *J. Chem. Thermodyn.* **43**, 948
2 (2011).
- 3 [16] S. I. Lall-Ramnarine, A. Castano, G. Subramaniam, M. F. Thomas, and J. F. Wishart, *Radiat.*
4 *Phys. Chem.* **78**, 1120 (2009).
- 5 [17] F. U. Shah, S. Glavatskih, D. R. MacFarlane, A. Somers, M. Forsyth, and O. N. Antzutkin,
6 *Phys. Chem. Chem. Phys.* **13**, 12865 (2011).
- 7 [18] H. K. Kashyap, C. S. Santos, H. V. Annapureddy, N. S. Murthy, C. J. Margulis, and E. W.
8 Castner Jr, *Faraday Discuss.* **154**, 133 (2012).
- 9 [19] J. J. Hettige, H. K. Kashyap, and C. J. Margulis, *J. Chem. Phys.* **140**, 111102 (2014).
- 10 [20] C. J. Bradaric, A. Downard, C. Kennedy, A. J. Robertson, and Y. Zhou, *Green Chem.* **5**, 143
11 (2003).
- 12 [21] F. Atefi, M. T. Garcia, R. D. Singer, and P. J. Scammells, *Green Chem.* **11**, 1595 (2009).
- 13 [22] M. Petkovic, D. O. Hartmann, G. Adamová, K. R. Seddon, L. P. N. Rebelo, and C. S. Pereira,
14 *New J. Chem.* **36**, 56 (2012).
- 15 [23] V. I. Pârvulescu and C. Hardacre, *Chem. Rev.* **107**, 2615 (2007).
- 16 [24] B. E. Gurkan, J. C. de la Fuente, E. M. Mindrup, L. E. Ficke, B. F. Goodrich, E. A. Price,
17 W. F. Schneider, and J. F. Brennecke, *J. Am. Chem. Soc.* **132**, 2116 (2010).
- 18 [25] H. Li, P. K. Cooper, A. E. Somers, M. W. Rutland, P. C. Howlett, M. Forsyth, and R. Atkin,
19 *J. Phys. Chem. Lett.* **5**, 4095 (2014).
- 20 [26] R. P. Swatloski, S. K. Spear, J. D. Holbrey, and R. D. Rogers, *J. Am. Chem. Soc.* **124**, 4974
21 (2002).
- 22 [27] L. C. Tomé, M. G. Freire, L. P. N. Rebelo, A. J. Silvestre, C. P. Neto, I. M. Marrucho, and
23 C. S. Freire, *Green Chem.* **13**, 2464 (2011).
- 24 [28] J. Zhang, S. Zhang, K. Dong, Y. Zhang, Y. Shen, and X. Lv, *Chem. Eur. J.* **12**, 4021 (2006).
- 25 [29] B. Gurkan, B. Goodrich, E. Mindrup, L. Ficke, M. Massel, S. Seo, T. Senftle, H. Wu, M. Glaser,
26 J. Shah, et al., *J. Phys. Chem. Lett.* **1**, 3494 (2010).
- 27 [30] B. F. Goodrich, J. C. de la Fuente, B. E. Gurkan, Z. K. Lopez, E. A. Price, Y. Huang, and
28 J. F. Brennecke, *J. Phys. Chem. B* **115**, 9140 (2011).
- 29 [31] S. Seo, M. Quiroz-Guzman, M. A. DeSilva, T. B. Lee, Y. Huang, B. F. Goodrich, W. F.
30 Schneider, and J. F. Brennecke, *J. Phys. Chem. B* **118**, 5740 (2014).
- 31 [32] R. E. Ramírez, L. C. Torres-González, and E. M. Sánchez, *J. Electrochem. Soc.* **154**, B229

- 1 (2007).
- 2 [33] K. Tsunashima and M. Sugiya, *Electrochem. Commun.* **9**, 2353 (2007).
- 3 [34] J. F. Jenck, F. Agterberg, and M. J. Droescher, *Green Chem.* **6**, 544 (2004).
- 4 [35] D. Thompson, S. Coleman, D. Diamond, and R. Byrne, *Phys. Chem. Chem. Phys.* **13**, 6156
5 (2011).
- 6 [36] F. Dommert and C. Holm, *Phys. Chem. Chem. Phys.* **15**, 2037 (2013).
- 7 [37] X. Liu, Y. Zhao, X. Zhang, G. Zhou, and S. Zhang, *J. Phys. Chem. B* **116**, 4934 (2012).
- 8 [38] Z. Liu, S. Huang, and W. Wang, *J. Phys. Chem. B* **108**, 12978 (2004).
- 9 [39] Y. Wang, S. Feng, and G. A. Voth, *J. Chem. Theory Comput.* **5**, 1091 (2009).
- 10 [40] H. A. Karimi-Varzaneh, F. Müller-Plathe, S. Balasubramanian, and P. Carbone, *Phys. Chem.
11 Chem. Phys.* **12**, 4714 (2010).
- 12 [41] D. Roy, N. Patel, S. Conte, and M. Maroncelli, *J. Phys. Chem. B* **114**, 8410 (2010).
- 13 [42] K. Wendler, F. Dommert, Y. Y. Zhao, R. Berger, C. Holm, and L. Delle Site, *Faraday Discuss.*
14 **154**, 111 (2012).
- 15 [43] Y.-L. Wang, A. Lyubartsev, Z.-Y. Lu, and A. Laaksonen, *Phys. Chem. Chem. Phys.* **15**, 7701
16 (2013).
- 17 [44] C. Spickermann, J. Thar, S. Lehmann, S. Zahn, J. Hunger, R. Buchner, P. Hunt, T. Welton,
18 and B. Kirchner, *J. Chem. Phys.* **129**, 104505 (2008).
- 19 [45] E. I. Izgorodina, U. L. Bernard, and D. R. MacFarlane, *J. Phys. Chem. A* **113**, 7064 (2009).
- 20 [46] C. J. Margulis, H. V. Annapureddy, P. M. De Biase, D. Coker, J. Kohanoff, and M. G.
21 Del Pópolo, *J. Am. Chem. Soc.* **133**, 20186 (2011).
- 22 [47] S. Chen, R. Vijayaraghavan, D. R. MacFarlane, and E. I. Izgorodina, *J. Phys. Chem. B* **117**,
23 3186 (2013).
- 24 [48] S. Zahn, D. R. MacFarlane, and E. I. Izgorodina, *Phys. Chem. Chem. Phys.* **15**, 13664 (2013).
- 25 [49] O. Hollóczki, F. Malberg, T. Welton, and B. Kirchner, *Phys. Chem. Chem. Phys.* **16**, 16880
26 (2014).
- 27 [50] C. Carlin and M. S. Gordon, *J. Comput. Chem.* **36**, 597 (2015).
- 28 [51] S. Vyas, C. Dreyer, J. Slingsby, D. Bicknase, J. M. Porter, and C. M. Maupin, *J. Phys. Chem.
29 A* **118**, 6873 (2014).
- 30 [52] A. Gupta, S. Sharma, and H. K. Kashyap, *J. Chem. Phys.* **142**, 134503 (2015).
- 31 [53] R. S. Payal and S. Balasubramanian, *Phys. Chem. Chem. Phys.* **16**, 17458 (2014).

- 1 [54] J. M. Araujo, A. B. Pereiro, J. N. Canongia Lopes, L. P. Rebelo, and I. M. Marrucho, *J. Phys.*
2 *Chem. B* **117**, 4109 (2013).
- 3 [55] J. N. Canongia Lopes and A. A. Pádua, *J. Phys. Chem. B* **110**, 19586 (2006).
- 4 [56] G. Zhou, X. Liu, S. Zhang, G. Yu, and H. He, *J. Phys. Chem. B* **111**, 7078 (2007).
- 5 [57] Y.-L. Wang, F. U. Shah, S. Glavatskih, O. N. Antzutkin, and A. Laaksonen, *J. Phys. Chem.*
6 *B* **118**, 8711 (2014).
- 7 [58] Y.-L. Wang, S. Sarman, S. Glavatskih, O. N. Antzutkin, M. W. Rutland, and A. Laaksonen,
8 *J. Phys. Chem. B* **119**, 5251 (2015).
- 9 [59] Y. Wang, S. Izvekov, T. Yan, and G. A. Voth, *J. Phys. Chem. B* **110**, 3564 (2006).
- 10 [60] B. L. Bhargava, R. Devane, M. L. Klein, and S. Balasubramanian, *Soft Matter* **3**, 1395 (2007).
- 11 [61] Z. Liu, X. Wu, and W. Wang, *Phys. Chem. Chem. Phys.* **8**, 1096 (2006).
- 12 [62] Z. Liu, T. Chen, A. Bell, and B. Smit, *J. Phys. Chem. B* **114**, 4572 (2010).
- 13 [63] X. Zhong, Z. Liu, and D. Cao, *J. Phys. Chem. B* **115**, 10027 (2011).
- 14 [64] T. Koller, J. Ramos, N. M. Garrido, A. P. Fröba, and I. G. Economou, *Mol. Phys.* **110**, 1115
15 (2012).
- 16 [65] M. G. Martin and J. I. Siepmann, *J. Phys. Chem. B* **102**, 2569 (1998).
- 17 [66] B. Chen and J. I. Siepmann, *J. Phys. Chem. B* **103**, 5370 (1999).
- 18 [67] G. Raabe and J. Köhler, *J. Chem. Phys.* **128**, 154509 (2008).
- 19 [68] X. Liu, G. Zhou, S. Zhang, and G. Yu, *Mol. Simul.* **36**, 79 (2010).
- 20 [69] S. Yeganegi, V. Sokhanvaran, and A. Soltanabadi, *Mol. Simul.* **39**, 1070 (2013).
- 21 [70] D. Reith, M. Pütz, and F. Müller-Plathe, *J. Comput. Chem.* **24**, 1624 (2003).
- 22 [71] A. Lyubartsev, A. Mirzoev, L. Chen, and A. Laaksonen, *Faraday Discuss.* **144**, 43 (2010).
- 23 [72] M. J. Frisch, G. W. Trucks, H. B. Schlegel, G. E. Scuseria, M. A. Robb, J. R. Cheeseman,
24 G. Scalmani, V. Barone, B. Mennucci, G. A. Petersson, et al., Gaussian Inc. Wallingford CT
25 (2009).
- 26 [73] M. Tosi and F. Fumi, *J. Phys. Chem. Solids* **25**, 45 (1964).
- 27 [74] J. C. Shelley, M. Y. Shelley, R. C. Reeder, S. Bandyopadhyay, and M. L. Klein, *J. Phys.*
28 *Chem. B* **105**, 4464 (2001).
- 29 [75] B. Hess, C. Kutzner, D. Van Der Spoel, and E. Lindahl, *J. Chem. Theory Comput.* **4**, 435
30 (2008).
- 31 [76] L. Laaksonen, *J. Mol. Graphics* **10**, 33 (1992).

- 1 [77] D. L. Bergman, L. Laaksonen, and A. Laaksonen, *J. Mol. Graphics Modell.* **15**, 301 (1997).
- 2 [78] J. Dwan, D. Durant, and K. Ghandi, *Cent. Eur. J. Chem.* **6**, 347 (2008).
- 3 [79] G. Adamová, R. L. Gardas, L. P. N. Rebelo, A. J. Robertson, and K. R. Seddon, *Dalton*
4 *Trans.* **40**, 12750 (2011).
- 5 [80] G. Adamová, R. L. Gardas, M. Nieuwenhuyzen, A. V. Puga, L. P. N. Rebelo, A. J. Robertson,
6 and K. R. Seddon, *Dalton Trans.* **41**, 8316 (2012).
- 7 [81] M. Quiroz-Guzman, D. P. Fagnant, X.-Y. Chen, C. Shi, J. F. Brennecke, G. S. Goff, and
8 W. Runde, *RSC Adv.* **4**, 14840 (2014).
- 9 [82] Y.-L. Wang, Z.-Y. Lu, and A. Laaksonen, *Phys. Chem. Chem. Phys.* **16**, 20731 (2014).
- 10 [83] H. Tokuda, K. Hayamizu, K. Ishii, M. A. B. H. Susan, and M. Watanabe, *J. Phys. Chem. B*
11 **108**, 16593 (2004).
- 12 [84] S. Sarman and A. Laaksonen, *Phys. Chem. Chem. Phys.* **17**, 3332 (2015).
- 13 [85] K. J. Fraser, E. I. Izgorodina, M. Forsyth, J. L. Scott, and D. R. MacFarlane, *Chem. Commun.*
14 pp. 3817–3819 (2007).